Journal of Alloys and Compounds 501 (2010) 198–203

Contents lists available at ScienceDirect

Journal of Alloys and Compounds

journal homepage: www.elsevier.com/locate/jallcom

Microstructure characterization of ball-mill prepared ternary $Ti_{0.9}Al_{0.1}C$ by X-ray diffraction and electron microscopy

H. Dutta [a], A. Sen [b], S.K. Pradhan [b,*]

[a] Department of Physics, Vivekananda College, Burdwan 713103, West Bengal, India
[b] Department of Physics, The University of Burdwan, Golapbag, Burdwan 713104, West Bengal, India

ARTICLE INFO

Article history:
Received 19 January 2010
Received in revised form 5 April 2010
Accepted 7 April 2010
Available online 22 April 2010

Keywords:
Nano-carbide
Ball-milling
Rietveld method
HRTEM

ABSTRACT

Synthesis of ternary carbide $Ti_{0.9}Al_{0.1}C$ by high energy ball-milling under argon atmosphere is investigated thoroughly. Microstructure characterization of ball-milled samples in terms of lattice imperfections and quantitative estimation of different phases present in the samples are done by using X-ray diffraction data employing Rietveld's powder structure refinement method. The results show that the formation of $Ti_{0.9}Al_{0.1}C$ nano-carbide starts after 48 min of ball-milling from Ti–Al–C solid solution. Full formation of $Ti_{0.9}Al_{0.1}C$ without any contaminated phase is achieved within 3 h of milling and to reduce particle size ball-milling is continued up to 10 h.

Direct observation of microstructure of 10 h ball-milled sample under high resolution TEM reveals supportive evidence of structural and microstructural evaluation by indirect method using XRD data.

1. Introduction

In recent years, metal carbides find high temperature structural applications because of their high melting temperature, high strength and ductility at high temperatures [1,2]. Among all of these metal carbides, as an important ceramic material, titanium aluminum carbide (Ti–Al–C) has recently gained increasing attention because it possesses unusual properties combining the merits of both metals and ceramics. It is thermally and electrically conductive, resistant to high-thermal shock, low density and easily machinable. In addition, it presents a high flexural strength, thermal stability and high temperature oxidation resistance. In contrast to the normal brittle ceramics, Ti–Al–C exhibits some abnormal room temperature compressive plasticity [3]. Such unique properties help this kind of materials to possess wide variety of potential applications in high-tech fields, e.g. elements of chemical equipment and abrasion resistant components. For example, it can be used as a high temperature structural material instead of expensive high temperature alloys, etc. Different technologies have been developed to fabricate Ti–Al–C composites, such as hot isostatic pressing (HIP), self propagation high temperature synthesis (SHS), combustion synthesis (CS), hot pressing (HP) and spark plasma sintering (SPS) [3–9]. All these above mentioned methods need rigorous conditions such as high pressure, high temperature and long time. Therefore, search for a new technology to prepare such an important material like Ti–Al–C composites in nanocrystalline form are still in progress.

High energy ball-milling also known as mechanical alloying (MA) is another technique and being utilized successfully in preparing materials those are very difficult to produce by any conventional method due to high melting temperatures of elements. Among several advantages, the chief advantage of MA renders a fine homogeneous nanocrystalline powder that can be consolidated and shaped according to a specific requirement by conventional powder metallurgy process. It has some other advantages, including low fabrication cost, simple synthetic method and easy industrialization. Recently, MA has been successfully used to synthesize various ceramic compounds or composites [10–12]. So far, research work in synthesize of Ti–Al–C powder using high energy ball-milling are very few in the literature [13]. In one of our recent works, we have synthesized nanocrystalline Ni_3C by ball-milling technique [14]. To avail potential advantages of high energy ball-milling in preparation of metal carbides in nanometric form, we have used this comparatively new technique for preparation of nanocrystalline Ti–Al–C starting from elemental blend of Ti, Al and graphite powders. Yang et al. reported the initiation of non-stoichiometric Ti_3AlC_2 composite after 3 h of milling with TiC contamination and after 10 h of milling they could prepare the TiC phase with Ti_3AlC_2 contamination [13]. We have prepared for the first time the Ti–Al–C composite (>0.95 mol fraction) within 48 min of milling followed by a mechanically induced self propagating reaction (MISPR) and it becomes stoichiometric $Ti_{0.9}Al_{0.1}C$ within 3 h of milling. In addition to that, we have characterized the microstructure of the prepared nano composite for the first time in terms of lattice imperfection of

* Corresponding author. Tel.: +91 342 2657800; fax: +91 342 2657800.
E-mail address: skp_bu@yahoo.com (S.K. Pradhan).

0925-8388/$ – see front matter © 2010 Elsevier B.V. All rights reserved.
doi:10.1016/j.jallcom.2010.04.101

different kinds. This article describes in detail the influence of lattice imperfections in the formation mechanism of Ti–Al–C phase within such a short duration of milling.

After full formation of the Ti–Al–C composite powder without any undesired contamination within 3 h ball-milling the powder was milled further up to 10 h to produce nanocrystalline single phase $Ti_{0.9}Al_{0.1}C$. Our next goal was to evaluate the microstructure in terms of lattice imperfections and quantitative estimation of different phases present in ball-milled powder materials employing the Rietveld's powder structure refinement analysis of X-ray powder diffraction data. In the present study, the Rietveld's analysis based on structure and microstructure refinement method [15–20] have been employed which is presumed to be the best method for microstructure characterization and quantitative estimation of multiphase nanocrystalline material containing significant number of overlapping reflections. Microstructure of 10 h milled sample has also been characterized by high resolution transmission electron microscope (HRTEM). Results obtained from both these analyses are in good agreement with each other.

2. Experimental

Pure titanium (M/s Alfa Aesar; purity 99.5%), aluminium (M/s Loba Chemie; purity 99.5%) and graphite (M/s Loba Chemie; purity 99.5%) powders were used as the starting ingredients and mixed in 0.45:0.05:0.5 molar ratio and then sealed in a chrome steel vial of 80 ml. volume together with chrome steel balls of 10 mm diameter in a glove box under Ar atmosphere. The ball-to-powder mass ratio (BPMR) was 40:1. The milling was performed at room temperature using a high energy planetary ball mill (Model-P5, M/s FRITSCH, GmbH, Germany). The milling was interrupted after a selected milling time and powder was collected from the vial. X-ray diffraction (XRD) with Ni-filtered CuK_α radiation from an X-ray powder diffractometer (Panalytical; Model PW1830) operated at 40 kV and 20 mA was used to monitor the structural changes of the milled powders at different interval of time varying from 48 min to 10 h. For detailed X-ray line profile analysis, step scan data (of step size 0.02° 2θ and counting time 30 s) of unmilled and all ball-milled samples were recorded for the entire angular range 20°–80° 2θ. HRTEM sample was prepared by conventional method [21]. The HRTEM images of 10 h ball-milled Ti–Al–C powders were taken from a TEM operated at 200 kV (Model HRTEM JEOL JEM 2100) for microstructure characterization of Ti–Al–C powder.

3. Microstructure evolution by X-ray diffraction

In the present study, we have adopted the Rietveld's powder structure refinement analysis [15–20] of X-ray powder diffraction step scan data to obtain the refined structural parameters and microstructural parameters, such as particle size and rms lattice strain using MAUD 2.12 [20] with pseudo-Voigt profile fitting function with asymmetry. To simulate the theoretical X-ray powder pattern α-Ti, Al, graphite and $Ti_{0.9}Al_{0.1}C$ phases in a single pattern are incorporated.

The Marquardt least-square procedures were adopted for minimization of the difference between the observed and simulated powder diffraction patterns and the minimization was carried out by using the reliability index parameter, R_{wp} (weighted residual error), R_B (Bragg factor) and R_{exp} (expected error) [15–20]. This leads to the value of goodness of fit [15–19]:

$$\text{GoF} = \frac{R_{wp}}{R_{exp}}$$

Refinement continues till convergence is reached with the value of the quality factor, GoF approaching 1, which confirms the goodness of refinement.

The Rietveld's method was successfully applied for determination of the quantitative phase abundances of the composite materials [22–25].

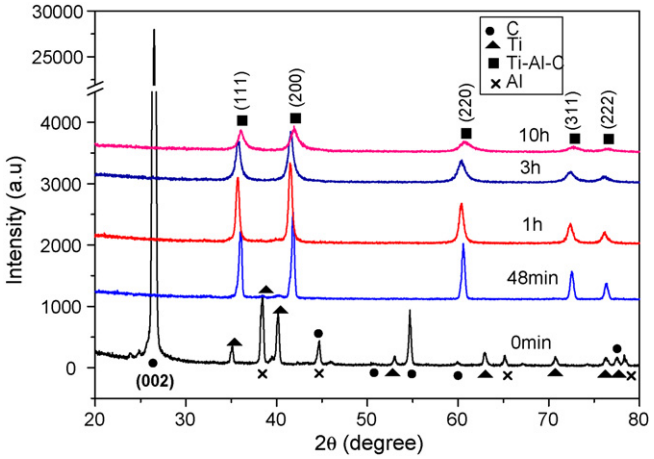

Fig. 1. X-ray powder diffraction patterns of unmilled and ball-milled Ti–Al–C powder mixtures. The peak positions of different phases are shown by different symbols in the figure.

4. Results and discussion

The X-ray powder diffraction patterns of unmilled and ball-milled powder mixture of the α-Ti, Al and graphite powders, milled at room temperature for different durations are shown in Fig. 1. It is clearly evident from the figure that all peaks in unmilled sample are quite sharp and high angle reflections are well resolved into Cu $K\alpha_1$–$K\alpha_2$ components, which indicates that all elements have quite large particle sizes and almost free from lattice strain. The relative intensity (r.i.) ratios of α-Ti (hcp) and Al (fcc) reflections are in accordance with the reported value (JCPDF file # 44-1294) and (JCPDF file # 04-0787) respectively but those of graphite (hexagonal) powder (JCPDF file # 41-1487) are extremely oriented along ⟨0 0 2⟩. This kind of preferred orientation leads to a major problem in determining the average particle size as well as the quantitative estimation of phases in a multiphase material. After just 48 min of milling, all α-Ti and Al reflections are almost absent in the XRD pattern. It is also noticed that all reflections of graphite powder disappear completely in the XRD pattern of 48 min ball-milled powder mixture. It can be seen that the formation of cubic $Ti_{0.9}Al_{0.1}C$ (similar to TiC, JCPDF File # 32-1383; S.G. *Fm*3*m*) phase is just happened after 48 min of milling through a mechanically induced self propagating reaction (MISPR). Though MISPR was observed earlier in several cases of metal carbide (TiC) formation [26–30], in the present case, the most probable reason for MISPR may be due to the fact that high energy ball-milling results in rapid decrease in particle size and thereby rapid accumulation of defects that lowers the activation energy for the reaction and brings the powder to a critical pre-combustion condition. The reaction can then be ignited easily by the energy of the colliding milling media. The high shock pressure experienced by powder trapped between colliding milling balls acts as the ignition of the reaction [31].

The $Ti_{0.9}Al_{0.1}C$ (fcc) powder formed after 48 min of milling via MISPR appears to be as an annealed standard material with clearly resolved Cu $K\alpha_1$–$K\alpha_2$ doublets even at lower scattering angle, having large grains without any lattice imperfection. To prepare nanocrystalline $Ti_{0.9}Al_{0.1}C$ powder, the as-prepared $Ti_{0.9}Al_{0.1}C$ powder with trace amount of unreacted Ti and Al powders after 48 min of milling was milled for longer durations. It is found that 3 h ball-milling results in full formation of stoichiometric $Ti_{0.9}Al_{0.1}C$ phase. XRD patterns of powder prepared at higher milling time appears with considerable amount of peak broadening and peak shifting, which increase continuously with increasing milling time.

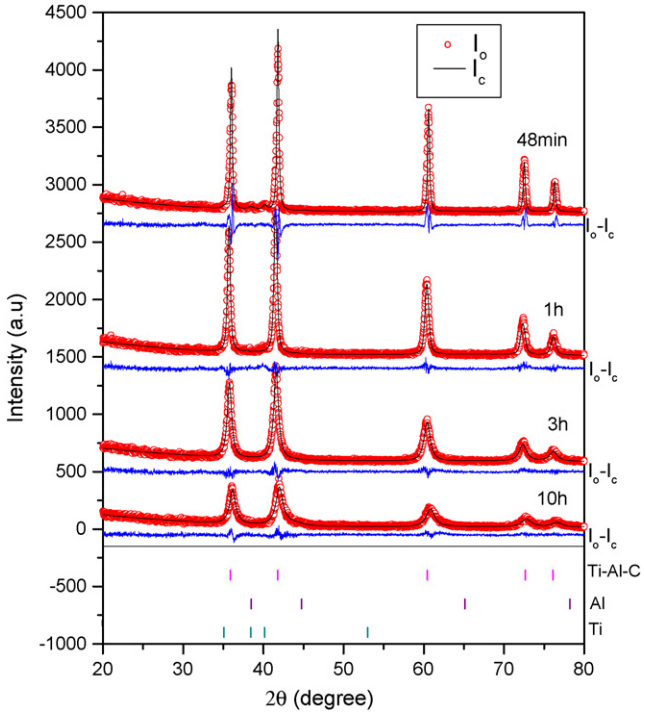

Fig. 2. Typical Rietveld output of X-ray powder diffraction patterns of ball-milled Ti–Al–C powder mixtures. Experimental data points are shown as hollow circles, while refined simulated patterns are shown as continuous lines. The difference between the experimental data (I_0) and the fitted simulated pattern (I_c) is shown as a continuous line ($I_0 - I_c$) under each diffraction pattern.

In the present study, Rietveld's structure and microstructure refinement method [15–20] has been employed for accurate estimation of phase contents and microstructure parameters of individual phases. All the experimental patterns (I_0) are fitted with the theoretically simulated patterns (I_c) and are shown in Fig. 2. Accuracy in fitting may be judged visually by examining the fitting residual ($I_0 - I_c$) of some of the fitted patterns plotted at the bottom of respective patterns in Fig. 2. Almost linear plots of residue except at the peak positions ensure that all the reflections of all phases have been fitted very well. The GoF values vary within 1.1–1.3 for fittings of all experimental data reveal that the simulated powder patterns are properly refined to fit the experimental powder patterns. Peak broadening of $Ti_{0.9}Al_{0.1}C$ reflections increases continuously with increasing milling time which is predominant in relatively higher milling time after full formation of $Ti_{0.9}Al_{0.1}C$ phase. This peak broadening is fitted very well by considering both the effect of small particle size and lattice strain, which are reasonably due to cold-working on $Ti_{0.9}Al_{0.1}C$ lattice during ball-milling.

Fig. 3 depicts the nature of variation of molar fraction of different phases with increasing milling time. Though α-Ti, Al and graphite powders were taken at molar ratio 0.45: 0.05: 0.5, but the Rietveld's analysis of unmilled sample reveals the ratio as ≈0.06: 0.11: 0.83 respectively. This significant change in composition arises due to highly oriented graphite layers along ⟨0 0 2⟩. Mol fraction of α-Ti and Al decreases rapidly within 48 min of milling and at the same time formation of $Ti_{0.9}Al_{0.1}C$ is noticed with a considerably high mol fraction value. Mol fraction of graphite becomes zero within 48 min of milling indicating graphite is completely used to form Ti–Al–C solid solution. It is interesting to note that mol fraction of Ti vanishes to zero in the milling time period between 48 min and 1 h but that of Al vanishes after 1 h of ball-milling. The formation of the $Ti_{0.9}Al_{0.1}C$ therefore can be interpreted as a result of formation of two types of solid solution, at first, interstitial solid solution of α-Ti–C and then substitutional solid solution Ti–Al–C due to accumulation of Al in the Ti–C matrix in course of milling. Nature of plot shows that mol fraction of $Ti_{0.9}Al_{0.1}C$ phase significantly increases after 1 h of ball-milling and this nature continues till 3 h of ball-milling in the time period of full formation of $Ti_{0.9}Al_{0.1}C$. Further ball-milling up to 10 h shows a linear nature indicating mol fraction of $Ti_{0.9}Al_{0.1}C$ phase reaches saturation condition (formation of single phase material contributing phase has mol fraction 1.0) after 3 h of milling.

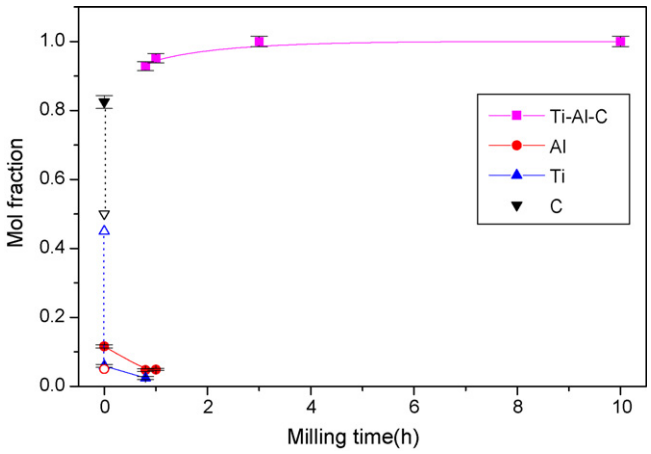

Fig. 3. Nature of variations of mol fractions of different phases obtained by ball-milling Ti–Al–C mixture powders with increasing milling time. True representation of mol fractions of different phases in unmilled powder are shown by dotted lines and hollow symbols.

Fig. 4 shows the variation of lattice parameters of the α-Ti, Al and Ti–Al–C phases obtained from Rietveld analysis. Lattice parameter of Al does not change significantly up to 48 min of milling but after then decreases rapidly. Contraction in lattice parameter of Al may be attributed to the formation of point defects and disorder in lattice in the process of MA. The increase in both α-Ti lattice parameters up to 48 min of milling confirms the inclusion of C-atoms into α-Ti matrix which results in formation of α-Ti–C interstitial solid solution as well as causes lattice expansion. On the way to preparation of nanocrystalline $Ti_{0.9}Al_{0.1}C$, its lattice parameter decreases very slowly and linearly up to 10 h of milling. This lattice contraction may be attributed to the formation of supersaturated solid solution as well as the point defects in the course of milling up to 10 h.

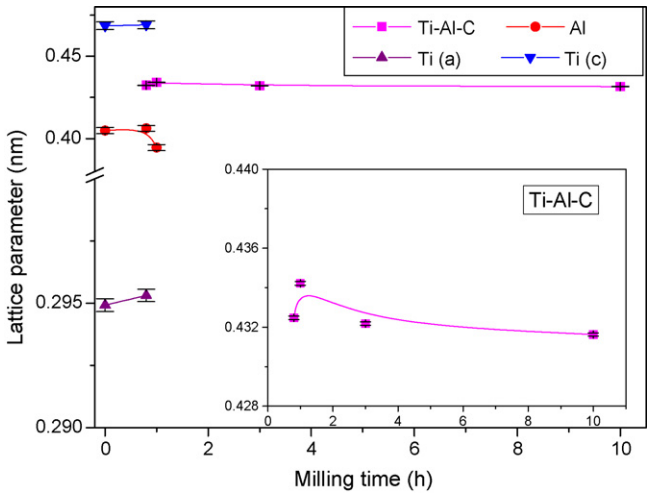

Fig. 4. Nature of variations of lattice parameters of different phases obtained by ball-milling Ti–Al–C mixture powders with increasing milling time. Inset: Variation of lattice parameters of Ti–Al–C with milling time.

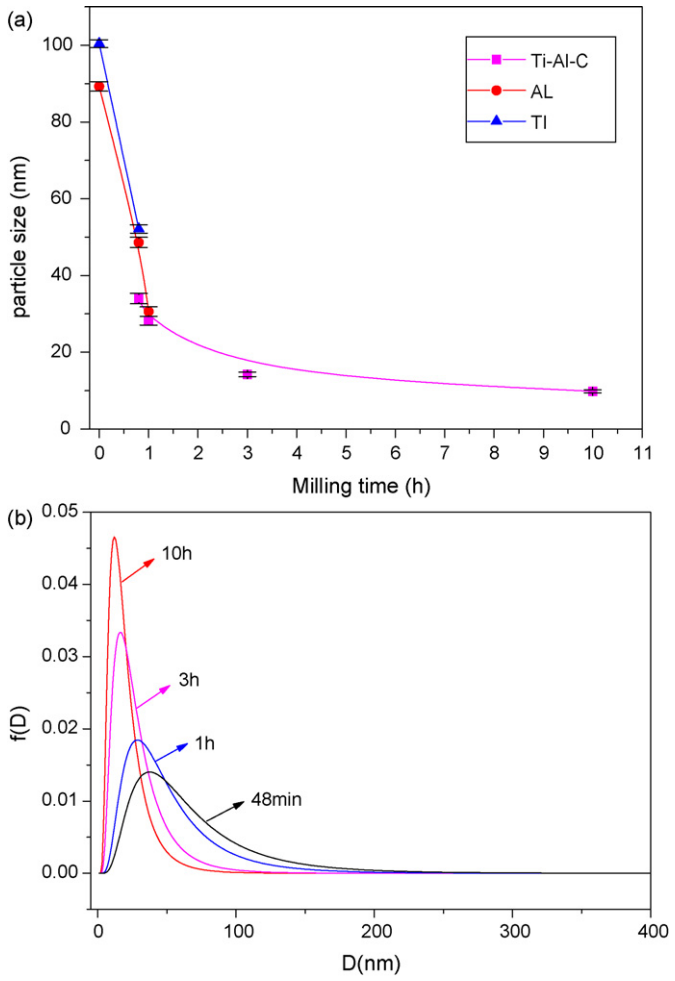

Fig. 5. Nature of variations of (a) particle sizes of different phases (b) size distribution of Ti–Al–C obtained by ball-milling Ti–Al–C mixture powders with increasing milling time.

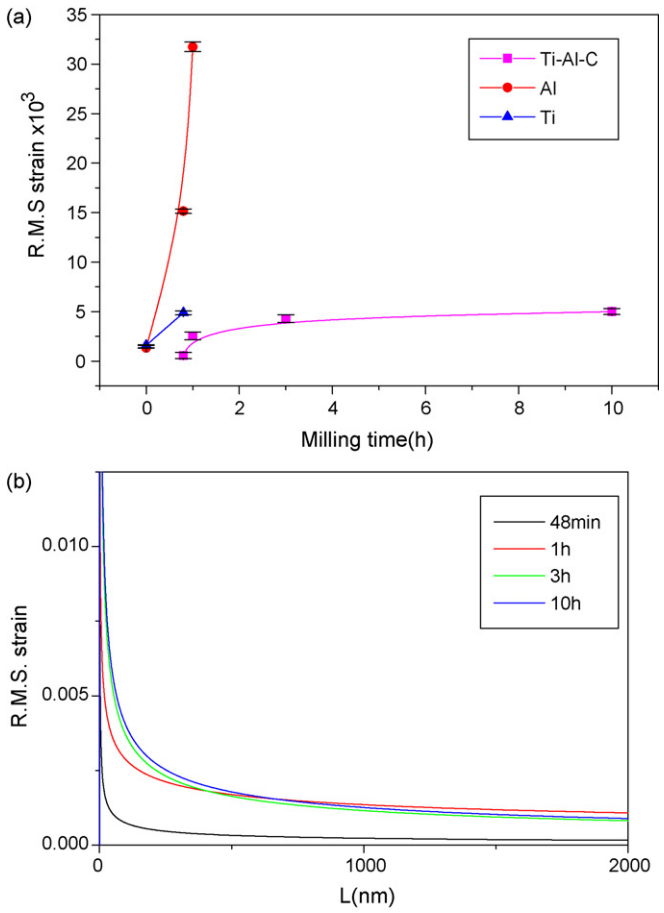

Fig. 6. Nature of variations of (a) r.m.s. strains of different phases (b) strain distribution of Ti–Al–C obtained by ball-milling Ti–Al–C mixture powders with increasing milling time.

Fig. 5(a) shows the variation of particle (coherently diffracting domain) size of α-Ti, Al and Ti–Al–C phases with increasing milling time, obtained from Rietveld analysis. All experimental profiles are fitted considering isotropic particle sizes of all the phases. However, the size distribution of $Ti_{0.9}Al_{0.1}C$ phase is particularly considered throughout the refinement process of different ball-milled samples and is depicted in Fig. 5(b). The particle size of α-Ti phase decreases rapidly from starting value ~100 nm to ~52 nm within 48 min of milling and that of Al phase reduces from ~90 nm to ~30 nm within 1 h of ball-milling (Fig. 5(a)). Due to the high temperature reaction of MISPR, particles of $Ti_{0.9}Al_{0.1}C$ phase grow with a relatively large size (~34 nm) after 48 min of milling, but reduces to ~28 nm within 1 h of milling. The 1 h ball-milled sample contains two phases, the major $Ti_{0.9}Al_{0.1}C$ (95 mol%) and minor Al (5 mol%) phase and both phases have nearly equal particle size values. After 1 h milling there is no trace of Al phase in the ball-milled sample indicating that particle size plays a vital role for diffusion of Al in α-Ti–C matrix

It is evident from variation of plots of Fig. 5(b) that the evenly dispersed $Ti_{0.9}Al_{0.1}C$ particles formed at 48 min of milling via combustion reaction (MISPR) have a relatively wide distribution of size with an average value ~34 nm. In the course of milling, the size distribution reduces continuously towards lower value. It is clearly evident from the plots that the most probable (peak maximum of the log normal distribution) particle size value of $Ti_{0.9}Al_{0.1}C$ decreases continuously with increasing milling time. This indicates that extensive ball-milling results in fracture the large particles and consequently both the size distribution and dispersion reduce substantially. Within 10 h of milling the average particle size of $Ti_{0.9}Al_{0.1}C$ reduces almost to10 nm with constant reduction of distribution. It means that by extension of ball-milling to a longer period, it is possible to prepare nanocrystalline $Ti_{0.9}Al_{0.1}C$ with almost uniform particle size.

Fig. 6(a) and (b) show variations of r.m.s. lattice strain of different phases and strain distribution of $Ti_{0.9}Al_{0.1}C$ in different milling time obtained from Rietveld analysis respectively. With increasing milling time, r.m.s. lattice strain of α-Ti and Al phases increase rapidly giving evidence that ball-milling introduces high strain in the produced powder material. The $Ti_{0.9}Al_{0.1}C$ phase is formed at 48 min of milling with nearly zero strain value. The strain value of $Ti_{0.9}Al_{0.1}C$ increases significantly within 3 h milling time i.e. more strain is accumulated in $Ti_{0.9}Al_{0.1}C$ matrix during the time of full formation of single $Ti_{0.9}Al_{0.1}C$ phase. This nature also shows that lattice strain is a crucial parameter for peak broadening in $Ti_{0.9}Al_{0.1}C$ reflections within 3 h of milling. After 3 h of ball-milling strain value variation of $Ti_{0.9}Al_{0.1}C$ shows a steady nature. After full formation of $Ti_{0.9}Al_{0.1}C$, strain value of the same phase remains almost unchanged even after 10 h of milling. It is evident from Fig. 6(b) that the lattice strains generated in $Ti_{0.9}Al_{0.1}C$ matrix during ball-milling are extended over a long period L ~200 nm ($L = na_3$, n is integer and a_3 is the lattice parameter) and increase continuously with increasing milling time. It may also be noted that the lattice strains are extended to a longer period with increasing milling time.

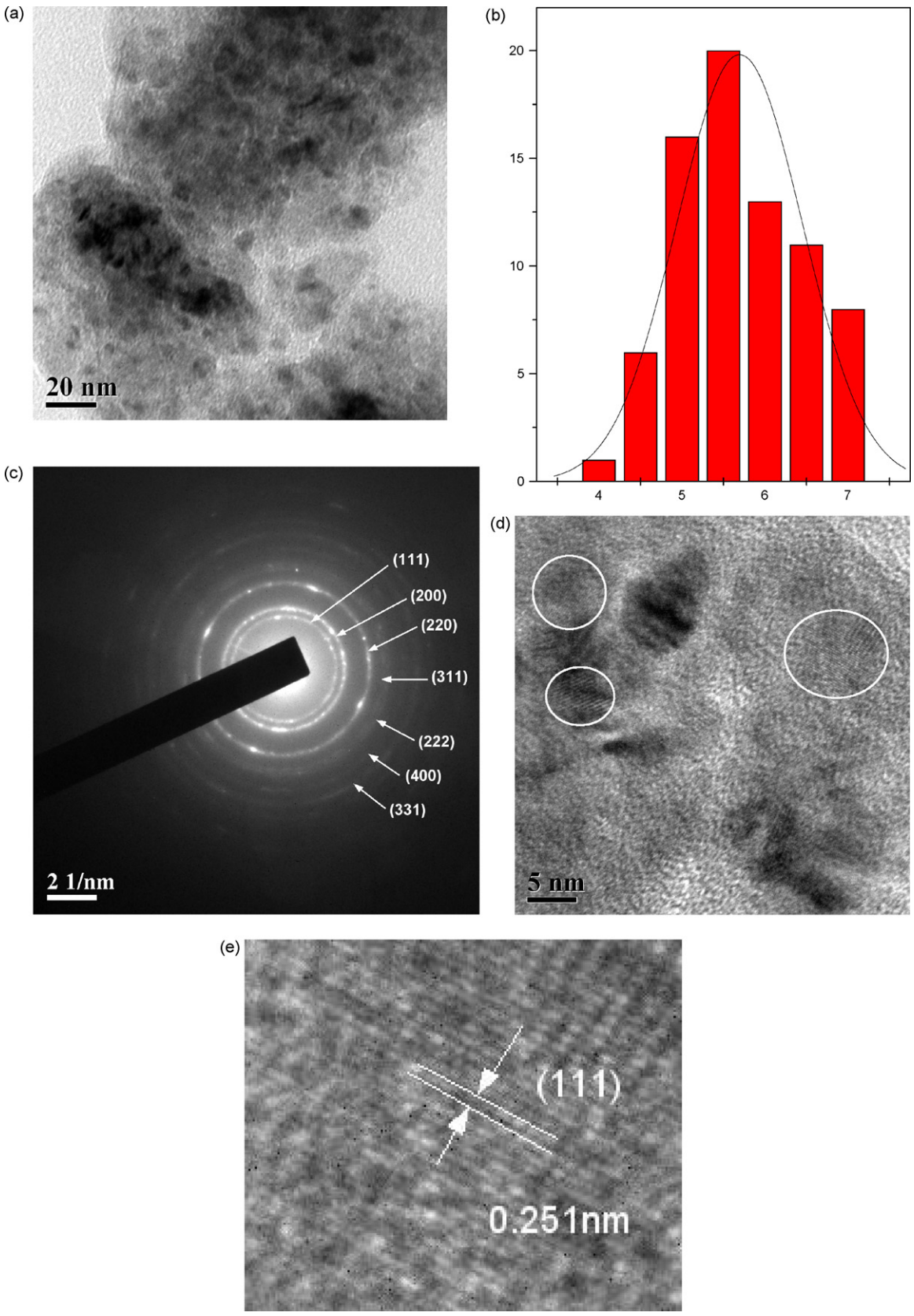

Fig. 7. HRTEM (a) transmission micrograph (b) histogram plot (c) diffraction pattern (d) Ti–Al–C nanoparticles and (e) micrograph containing (1 1 1) planes in a nanocrystalline particle of 10 h ball-milled homogeneous mixture of Ti–Al–C powders.

The HRTEM image of 10 h ball-milling sample and histogram of particle size distribution obtained from HRTEM images analysis are shown in Fig. 7(a) and (b) respectively. The shape of $Ti_{0.9}Al_{0.1}C$ particles are found to be almost isotropic in nature with a size distribution ~5–6 nm which is of same order of magnitude as found from XRD analysis by Rietveld analysis. The indexed selected area electron diffraction (SAED) pattern in Fig. 7(c) clearly reveals only the presence of cubic $Ti_{0.9}Al_{0.1}C$ phase in 10 h milled sample. We have clearly noticed the $Ti_{0.9}Al_{0.1}C$ nanoparticles in HRTEM image (marked by white rings in Fig. 7(d)) and a selected portion of that image is magnified and shown in Fig. 7(e). Interplanar spacing of these planes of a nanocrystalline particle is calculated from Fig. 7(e) and the value 0.251 nm corresponds to the (1 1 1) planes also gives a direct evidence of full formation of cubic $Ti_{0.9}Al_{0.1}C$ phase in 10 h milled sample.

5. Conclusions

In our present study ternary carbide $Ti_{0.9}Al_{0.1}C$ has been prepared by high energy ball-milling the elemental α-Ti, Al, and graphite powders under argon atmosphere. We have noticed the formation of Ti–Al–C phase after 48 min of milling and full formation of single phase nanocrystalline $Ti_{0.9}Al_{0.1}C$ after 3 h ball-milling. Detailed microstructure characterization in terms of lattice imperfections is done by analyzing XRD data employing Rietveld method. HRTEM analysis gives supportive evidence of the findings of X-ray analysis in case of particle size value and phase identification.

Acknowledgement

One of the authors, HD, wishes to thank the University Grant Commission (UGC) India, for granting financial assistant in “minor research project”. Another author, SKP, wishes to thank the University Grant Commission (UGC) India, for granting DSA–III programme under the thrust area “Condensed Matter Physics including Laser applications” to the Department of Physics, The University of Burdwan under the financial assistance of which the work has been carried out. We are also grateful to IIT, KGP for providing the HRTEM facility.

References

[1] M. Le Flem, A. Allemand, S. Urvoy, D. Cedat, C. Rey, J. Nucl. Mater. 380 (2008) 85–92.
[2] Z. Xinkun, Z. Kunyu, C. Baochang, L. Qiushi, Z. Xiuqin, C. Tieli, S. Yunsheng, Mater. Sci. Eng. C 16 (2001) 103–105.
[3] N.V. Tzenov, M.W. Barsoum, J. Am. Ceram. Soc. 83 (2000) 825–832.
[4] C.L. Yeh, Y.G. Shen, J. Alloys Compd. 466 (2008) 308–313.
[5] Z. Weibing, M. Bingchu, Z. Jiaoqun, Ceram. Int. 35 (2009) 3507–3510.
[6] A. Hendaoui, D. Vrel, A. Amara, P. Langlois, M. Andasmas, M. Guerioune, J. Eur. Ceram. Soc. 30 (2010) 1049–1057.
[7] C. Yang, S. Jin, B. Liang, G. Liu, L. Duan, S. Jia, J. Alloys Compd. 472 (2009) 79–83.
[8] C.L. Yeh, Y.G. Shen, J. Alloys Compd. 482 (2009) 219–223.
[9] S.-H. Chang, Mater. Trans. 50 (2009) 909–916.
[10] A. Gajović, I. Djerdj, K. Furić, R. Schlögl, D.S. Su, Cryst. Res. Technol. 41 (2006) 1076–1081.
[11] S. Bid, P. Sahu, S.K. Pradhan, Physica E 39 (2007) 175–184.
[12] S.K. Pradhan, H. Dutta, Physica E 27 (2005) 405–419.
[13] C. Yang, S.Z. Jin, B.Y. Liang, G.J. Liu, S.S. Jia, J. Mater. Process. Technol. 209 (2009) 871–875.
[14] B. Ghosh, H. Dutta, S.K. Pradhan, J. Alloys Compd. 479 (2009) 193–200.
[15] L. Lutterotti, P. Scardi, P. Maistrelli, J. Appl. Crystallogr. 25 (1992) 459–462.
[16] H.M. Rietveld, Acta Crystallogr. 22 (1967) 151–152.
[17] H.M. Rietveld, J. Appl. Crystallogr. 2. (1969) 65–71.
[18] R.A. Young, D.B. Wiles, J. Appl. Crystallogr. 15 (1982) 430–438.
[19] M. Sinha, H. Dutta, S.K. Pradhan, Jpn. J. Appl. Phys. 47 (2008) 8667–8672.
[20] L. Lutterotti, Maud version 2.074, 2009 http://www.ing.unitn.it/~maud/.
[21] S. Patra, B. Satpati, S.K. Pradhan, J. Appl. Phys. 106 (2009), 034313–1–8.
[22] H. Toraya, J. Appl. Cryst. 33 (2000) 1324–1328.
[23] H. Dutta, S.K. Manik, S.K. Pradhan, J. Appl. Crystallogr. 36 (2003) 260–268.
[24] H. Dutta, M. Sinha, Y.-C. Lee, S.K. Pradhan, Mater. Chem. Phys. 105 (2007) 31–37.
[25] A. Gajoviĭc, N. Toma˘siĭc, I. Djerdj, D.S. Su, K. Furiĭc, J. Alloys Compd. 456 (2008) 313–319.
[26] N.Q. Wu, S. Lin, J.M. Wu, Z.Z. Li, J. Mater. Sci. Technol. 14 (1998) 287–291.
[27] Z. Xinkun, C. Baochang, L. Quishi, Z. Xiuquin, C. Tieli, S. Yunsheng, Mater. Sci. Eng. C 16 (2001) 103–105.
[28] C. Deidda, S. Doppiu, M. Monagheddu, G. Cocco, J. Metastable Nanocryst. Mater. 15–16 (2003) 215–220.
[29] B.H. Loshe, A. Calka, D. Wexler, J. Alloys Compd. 394 (2005) 148–151.
[30] B.H. Loshe, A. Calka, D. Wexler, J. Mater. Sci. 42 (2007) 669–675.
[31] W.H. Lee, P.J. Reucroft, C.S. Byun, D.K. Kim, J. Mater. Sci. Lett. 20 (2001) 1647–1649.